

Article

Infrared Dissimilar Joining of Ti₅₀Ni₅₀ and 316L Stainless Steel with Copper Barrier Layer in between Two Silver-Based Fillers

Ren-Kae Shiue ¹, Shyi-Kaan Wu ^{1,2,*}, Sheng-Hao Yang ² and Chun-Kai Liu ²

¹ Department of Materials Science and Engineering, National Taiwan University, Taipei 106, Taiwan; rkshiue@ntu.edu.tw

² Department of Mechanical Engineering, National Taiwan University, Taipei 106, Taiwan; r02522707@ntu.edu.tw (S.-H.Y.); r03522731@ntu.edu.tw (C.-K.L.)

* Correspondence: skw@ntu.edu.tw; Tel.: +886-23-366-2732

Received: 1 July 2017; Accepted: 17 July 2017; Published: 18 July 2017

Abstract: Infrared dissimilar joining Ti₅₀Ni₅₀ and 316L stainless steel using Cu foil in between Cusil-ABA and BAg-8 filler metals has been studied. The Cu foil serves as a barrier layer with thicknesses of 70 μm and 50 μm , and it successfully isolates the interfacial reaction between Ti and Fe at the 316L SS (stainless steel) substrate side. In contrast, the Cu foil with 25 μm in thickness is completely dissolved into the braze melt during brazing and fails to be a barrier layer. A layer of (Cu_xNi_{1-x})₂Ti intermetallic is formed at the Ti₅₀Ni₅₀ substrate side, and the Cu interlayer is dissolved into the Cusil-ABA melt to form a few proeutectic Cu particles for all specimens. For the 316L SS substrate side, no interfacial layer is observed and (Ag, Cu) eutectic dominates the brazed joint for 70 μm /50 μm Cu foil. The average shear strength of the bond with Cu barrier layer is greatly increased compared with that without Cu. The brazed joints with a 50 μm Cu layer demonstrate the highest average shear strengths of 354 MPa and 349 MPa for samples joined at 820 °C and 850 °C, respectively. Cracks are initiated/propagated in (Ag, Cu) eutectic next to the 316L substrate side featured with ductile dimple fracture. It shows great potential for industrial application.

Keywords: shape memory alloy; stainless steel; barrier layer; infrared brazing; microstructure

1. Introduction

Equal atomic TiNi shape memory alloy (SMA) is one of the best and intensively studied SMAs with excellent shape memory properties [1,2]. At present, equiatomic TiNi SMA has many industrial applications, such as mechanical actuators and micro sensors in intelligent material systems [3,4]. AISI (American Iron and Steel Institute) 316L stainless steel (316L SS) has the chemical composition in wt % of Fe-0.03C-17Cr-12Ni-2.5Mo and exhibits high oxidation and corrosion resistance [5]. Joining of Ti₅₀Ni₅₀ SMA and 316L SS has the opportunity for industrial applications. For instance, shape-memory actuators are used to replace exploding bolts utilized in petrochemical equipment and nuclear power plants [6]. The shape-memory actuator is joined with an infrastructure made of stainless steel or nickel-based alloy. In our reported study, dissimilar joining of Ti₅₀Ni₅₀ SMA and 316L SS by infrared brazing using two Ag-based filler metals, Ticusil (Ag-26.7Cu-4.5Ti, wt %) and Cusil-ABA (Ag-35.25Cu-1.75Ti, wt %), was evaluated [6]. Test results demonstrated that the maximum joining strength of 237 MPa shear stress can be obtained for Ticusil filler brazed at 950 °C for 60 s, and 66 MPa for Cusil-ABA one joined at 870 °C for 300 s. The formation of Ti-Fe-(Cr) interfacial layer was found to be detrimental to all joint strengths [6].

Dissimilar joining of Ti and many engineering alloys has been extensively studied in recent years [7–9]. Titanium (Ti) alloys directly bonded to SS will form TiFe/TiFe₂ intermetallics and result

in inherent brittleness of the joint [10–12]. For avoiding the occurrence of brittle intermetallics, an interlayer of diffusion barrier was proposed to add in between the joining substrates [13–15]. A nickel interlayer with 30 μm in thickness had been used as a diffusion barrier in diffusion bonding of 304 SS and Ti-6Al-4V, so a robust joint was obtained [16]. A nickel barrier layer was also used to braze 17-4 PH (precipitation hardened) SS and Ti-6Al-4V successfully [17]. However, although the nickel interlayer can avoid the formation of brittle TiFe/TiFe₂ intermetallics in brazing the Ti alloy and SS, but another brittle one, such as TiNi₃, can occur in the joint. Therefore, the nickel interlayer may be not the best choice for the diffusion barrier in brazing Ti₅₀Ni₅₀ SMA and 316L SS, because Ti₅₀Ni₅₀ substrate can provide Ti and Ni atoms to enhance the brittle Ti-Ni intermetallic(s) to form.

It is well known that the solubility of Fe in Cu is very low [18]. In addition, the interfacial reaction of Ti₅₀Ni₅₀ SMA and Cusil-ABA/Ticusil filler metals forms a TiNiCu intermetallic in the Ti₅₀Ni₅₀ substrate side, and this intermetallic is regarded as not so brittle [6,19]. Thus, an interlayer of Cu foil can be selected as a diffusion barrier in between Cusil-ABA and BAg-8 filler metals to prevent the interaction between Ti and Fe atoms in brazing Ti₅₀Ni₅₀ SMA and 316L SS. The Cusil-ABA filler metal has good wettability with Ti₅₀Ni₅₀ SMA and thus is chosen to contact with Ti₅₀Ni₅₀ substrate [6]. BAg-8 filler metal is selected to neighbor the 316L SS substrate due having no Ti atom to form brittle Ti-Fe intermetallic(s) at the 316L SS substrate side, although the wettability of BAg-8 one with 316L SS is not so good [20].

The alloys' joining brazed by an infrared power source can quickly heat up the specimen with a maximum heating rate of 50 $^{\circ}\text{C}/\text{s}$, and it is much faster than that of ordinary electric furnace [21,22]. Under the condition of temperature being precisely controlled, the joining process by infrared brazing is quite suitable to investigate the early-stage evolution of the reaction kinetics exhibited in the brazed joint. Therefore, microstructural evolution, metallurgical reaction, and bonding strength of brazed joints under different brazing variables have been extensively evaluated.

2. Materials Used and Experimental Procedure

Equal atomic TiNi SMA used in the experiment was prepared from titanium and nickel pellets (both with 99.9 wt % purity) with six times remelting in the vacuum arc remelter (Series 5 Bell Jar, Centorr Vacuum Ind., Nashua, NH, USA) under pure argon gas. The solution-treated Ti₅₀Ni₅₀ sample was cut by a diamond saw into small templates at a size of 15 mm \times 15 mm \times 3 mm for metallographical observations, and 15 mm \times 7 mm \times 4 mm for shear tests. The surface used for brazing was ground and polished by SiC papers and Al₂O₃ suspension solution, and then cleaned in an ultrasonic acetone container. Foils of Cusil-ABA, BAg-8, and Cu fillers were all purchased from Wesgo Metals (Hayward, CA, USA), and the former two foils' thickness was 50 μm and those of Cu foils were 25 μm , 50 μm , and 75 μm for comparison. Table 1 lists chemical compositions and melting temperatures of three filler foils.

In the experiment, infrared heating was used to braze Ti₅₀Ni₅₀ SMA and 316L SS using a Cu barrier layer in between Cusil-ABA (active braze alloy) and BAg-8 filler metals, as shown in Figure 1. An infrared heating furnace made from ULVAC Company (Tokyo, Japan) with the model of RHL-P816C was utilized as the main component. The furnace was kept at 5×10^{-5} mbar vacuum and set at 15 $^{\circ}\text{C}/\text{s}$ heating rate in the test. Figure 2 shows the schematic diagram of infrared brazing furnace. Graphite holders on both substrates were used to increase the infrared ray absorption on the specimen. The dissimilar brazed sample was preheated at 700 $^{\circ}\text{C}$ for 300 s before infrared brazing in order to equilibrate thermal gradient of the brazed sample. 820 $^{\circ}\text{C}$ and 850 $^{\circ}\text{C}$ for 300 s were selected as the brazing condition.

Table 1. Compositions and melting behaviors of three filler foils.

Braze Foil	Cusil-ABA	BAg-8	Copper
Chemical composition	63Ag-35.25Cu-1.75Ti (wt %)	72Ag-28Cu (wt %)	99.95% purity (wt %)
Solidus temperature	780 °C	780 °C	1083 °C
Liquidus temperature	815 °C	780 °C	1083 °C

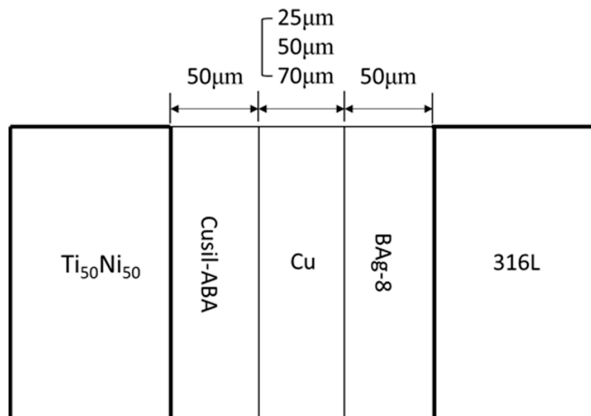


Figure 1. The schematic diagram shows the infrared brazed Ti₅₀Ni₅₀ SMA/Cusil-ABA/Cu foil/BAg-8/316L SS joint. Thicknesses of the copper foils are 25, 50, 70 µm and those of Cusil-ABA and BAg-8 filler metals are 50 µm; SMA: shape memory alloy; ABA: active braze alloy.

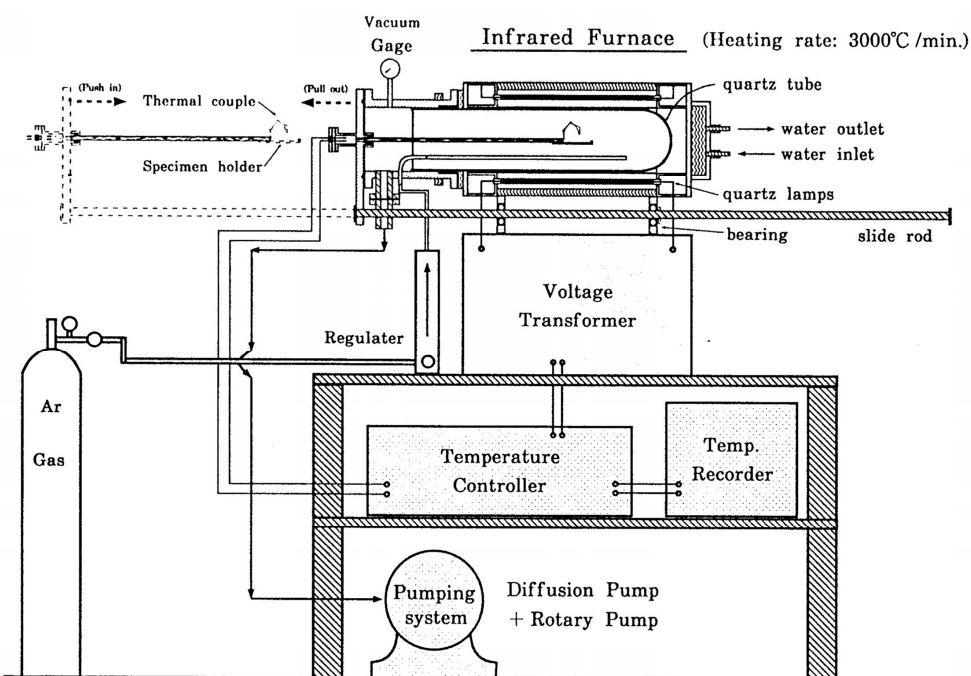


Figure 2. The schematic diagram of infrared brazing furnace.

To evaluate joint strength of the brazed sample in this study, shear tests were conducted with three specimens being performed in each brazing condition. According to our past experience, a double lap joint of 316L SS/Ti₅₀Ni₅₀/316L SS was used in shear test [21,22]. A Shimadzu universal testing machine with AG-10 model was used to conduct shear tests with a strain rate of 0.0167 mm/s. For the microstructural observations, the cross-section of infrared brazed joints were cut and then prepared by standard metallographic procedures, thereafter examined using a scanning electron microscope (SEM) with NOVA NANO 450 model.

3. Experimental Results and Discussion

3.1. Microstructures of Brazed Joints

Figure 3 and Table 2 show the cross-sectional results of SEM backscattered electron images (BEIs) and energy dispersive spectroscope (EDS) chemical analysis results of Ti₅₀Ni₅₀/Cusil-ABA/70 μm Cu foil/BAg-8/316L SS specimens brazed by infrared rays at 820 °C for 300 s. In EDS analyses, the electron beam in a point with 1 μm in diameter was used for all single phase analysis, and a larger beam diameter of 5 μm was applied for eutectic analysis as marked by D in Figure 3. Figure 3a illustrates the cross-sectional SEM BEIs results, in which the area on the Ti₅₀Ni₅₀ side and that on the 316L SS side are displayed in Figure 3b,c, respectively. From Figure 3a, the thickness of the Cu interlayer is about 70 μm (labelled by C and F). The layer marked by C in the left side of the Cu interlayer contains 90.5 at % Cu and has some Cu atoms dissolved into Cusil-ABA melt to form the proeutectic Cu (labelled by G in Figure 3b). Figure 3b indicates that a layer of (Cu_xNi_{1-x})₂Ti intermetallic (labelled by B) is formed at the interface of Cusil-ABA filler and Ti₅₀Ni₅₀ base metal. It is similar to the Ti₅₀Ni₅₀ side of 316L SS/Cusil-ABA/Ti₅₀Ni₅₀ joint brazed by infrared rays at 870 °C and 900 °C for 300 s [6]. In contrast, there is no interaction layer formed in between the BAg-8 braze and the 316L SS substrate, as displayed in Figure 3c. The Cu interlayer is dissolved into both molten brazes resulting in irregular interfaces among Cu and two brazes.

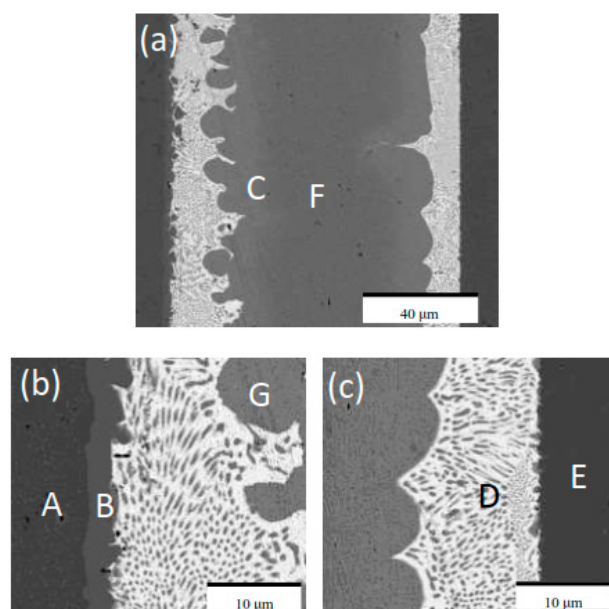


Figure 3. SEM (scanning electron microscope) backscattered electron images (BEIs) of Ti₅₀Ni₅₀/Cusil-ABA/70 μm Cu foil/BAg-8/316L SS specimen infrared brazed at 820 °C for 300 s: (a) the cross-section; (b) the Ti₅₀Ni₅₀ substrate side; (c) the 316L SS substrate side.

Table 2. EDS chemical analysis results in Figure 3.

at %	A	B	C	D	E	F	G
Ti	49.8	30.7	3.9	-	-	-	2.5
Cu	-	51.6	90.5	47.2	-	100	89.3
Ni	50.2	17.7	-	-	10.8	-	-
Fe	-	-	-	-	68.1	-	-
Ag	-	-	5.6	52.8	-	-	8.2
Cr	-	-	-	-	21.1	-	-
Phase	Ti ₅₀ Ni ₅₀	(Cu _x Ni _{1-x}) ₂ Ti	Cu-rich	Ag-Cu eutectic	316L	Cu	Cu-rich

The thickness effect of the Cu barrier layer on the infrared brazed joint was studied. Figure 4 displays SEM BEIs cross sections of Ti₅₀Ni₅₀/Cusil-ABA/Cu/BAg-8/316L SS specimens brazed by infrared rays at 850 °C for 300 s with various thicknesses of the Cu interlayer. From Figure 4a, one can find that the continuous Cu barrier layer disappears and replaced by many huge proeutectic Cu-rich blocks. In contrast, the thickness of Cu barrier layer above 50 µm is enough to isolate the interaction between Ti₅₀Ni₅₀ and 316L SS, as illustrated in Figure 4b,c. The dissolution of Cu barrier layer into Cusil-ABA melt becomes more prominent in Figure 4c than that in Figure 3a due to the higher brazing temperature. Additionally, one can find that the width of BAg-8 melt (in the right side of the Cu interlayer) in Figure 4c is less than that in Figure 3a, since BAg-8 melt flows out of the joint during brazing at a higher temperature. According to Table 1, the BAg-8 eutectic temperature is less than the liquidus temperature of Cusil-ABA braze. The width of BAg-8 filler is significantly decreased with increasing the brazing temperature.

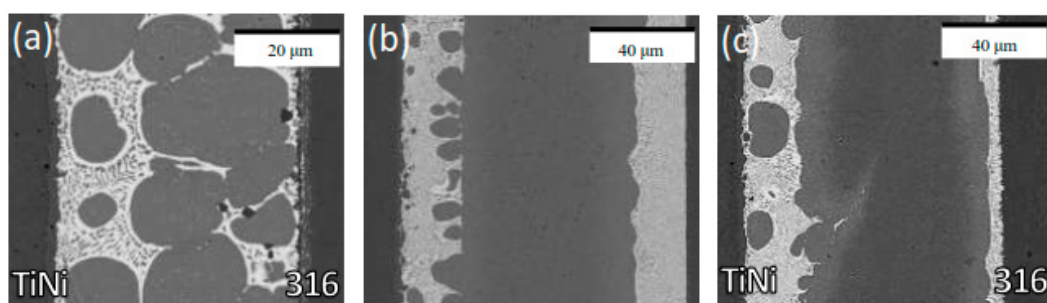


Figure 4. SEM BEI cross sections of Ti₅₀Ni₅₀/Cusil-ABA/Cu/BAg-8/316L SS specimens infrared brazed at 850 °C for 300 s with the Cu interlayer of (a) 25 µm; (b) 50 µm; (c) 70 µm. (TiNi: Ti₅₀Ni₅₀ substrate, 316: 316L SS substrate).

Figure 5 and Table 3 illustrate the cross-sectional results of SEM BEIs and EDS chemical analyses of Ti₅₀Ni₅₀/Cusil-ABA/25 µm Cu foil/BAg-8/316L SS specimen brazed by infrared rays at 850 °C for 300 s. Figure 5a,b indicate the area on the Ti₅₀Ni₅₀ side and that on 316L SS side, respectively. In Figure 5a, a (Cu_xNi_{1-x})₂Ti intermetallic layer (labelled by B) is formed at the Ti₅₀Ni₅₀ side which is similar to that in Figure 3b [6,20,22]. The silver penetrated into the (Cu_xNi_{1-x})₂Ti layer is also observed. According to Figure 5b, two interfacial layers are formed at the 316L SS side, one is Ti(Fe, Ni) intermetallic layer (labelled by D), and the other is regarded as a layer of (Fe, Cr)-rich phase (labelled by E) [6]. The existence of continuous Ti(Fe, Ni) reaction layer will be discussed later. Both D and E layers have silver agglomerations (white spots in Figure 5b) with the layer E having more. In addition, there is a TiCu precipitate in the braze, as labelled by G in Figure 5b [19]. The existence of the Ti-Fe interfacial layer in Figure 5b is quite dissimilar to that in Figure 3c. Because the 25 µm Cu barrier layer is completely dissolved into the braze melt, Ti atoms transport into the 316L SS side forming the interfacial Ti(Fe, Ni) intermetallic layer [6].

Figure 6 and Table 4 display the cross-sectional inspection of SEM BEIs and EDS analyses of Ti₅₀Ni₅₀/Cusil-ABA/50 µm Cu foil/BAg-8/316L SS specimen brazed by infrared rays at 850 °C for 300 s. Interfacial reactions shown in Figure 6 are similar to those in Figure 3. Additionally, the experimental results of the infrared brazed Ti₅₀Ni₅₀/Cusil-ABA/Cu foil/BAg-8/316L SS joint with 70 µm thickness of the Cu foil at 850 °C are similar to those of the 50 µm one illustrated in Figure 6, and therefore are not shown here.

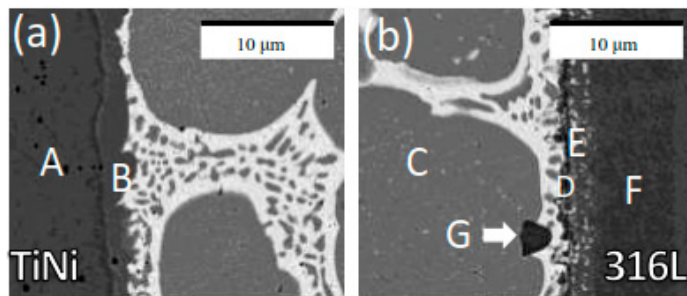


Figure 5. SEM BEI cross sections of $\text{Ti}_{50}\text{Ni}_{50}$ /Cusil-ABA/25 μm Cu foil/BAg-8/316L SS specimen infrared brazed at 850 $^{\circ}\text{C}$ for 300 s: (a) the $\text{Ti}_{50}\text{Ni}_{50}$ substrate side; (b) the 316L SS substrate side. (TiNi: $\text{Ti}_{50}\text{Ni}_{50}$ substrate, 316L: 316L SS substrate).

Table 3. EDS chemical analysis results in Figure 5.

at %	A	B	C	D	E	F	G
Ti	50.2	31.6	2.2	40.0	9.9	-	50.1
Cu	-	49.8	92.6	4.8	-	-	46.4
Ni	49.8	18.6	-	12.7	3.3	10.5	3.5
Fe	-	-	-	37.0	56.1	69.1	-
Ag	-	-	5.2	2.9	9.1	-	-
Cr	-	-	-	2.6	21.6	20.4	-
Phase	$\text{Ti}_{50}\text{Ni}_{50}$	$(\text{Cu}_x\text{Ni}_{1-x})_2\text{Ti}$	Cu-rich	$\text{Ti}(\text{Fe}, \text{Ni})$	(Fe, Cr)-rich	316L	TiCu

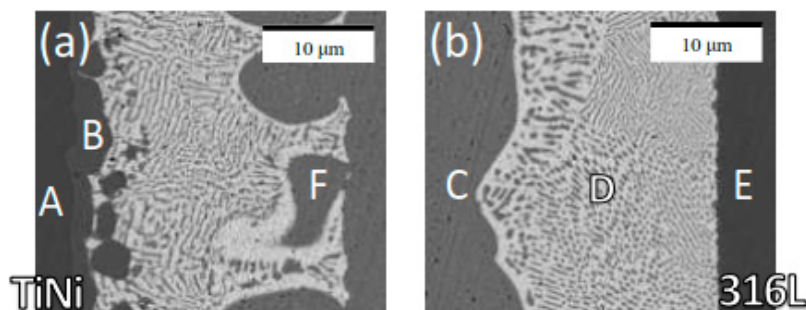


Figure 6. SEM BEI cross sections of $\text{Ti}_{50}\text{Ni}_{50}$ /Cusil-ABA/50 μm Cu foil/BAg-8/316L SS specimen infrared brazed at 850 $^{\circ}\text{C}$ for 300 s: (a) the $\text{Ti}_{50}\text{Ni}_{50}$ substrate side; (b) the 316L SS substrate side. (TiNi: $\text{Ti}_{50}\text{Ni}_{50}$ substrate, 316L: 316L SS substrate).

Table 4. EDS chemical analysis results in Figure 6.

at %	A	B	C	D	E	F
Ti	49.7	30.6	-	-	-	4.5
Cu	-	48.6	100	27.7	-	90.4
Ni	50.3	20.8	-	-	13.1	-
Fe	-	-	-	-	68.9	-
Ag	-	-	-	72.3	-	5.1
Cr	-	-	-	-	18.0	-
Phase	$\text{Ti}_{50}\text{Ni}_{50}$	$(\text{Cu}_x\text{Ni}_{1-x})_2\text{Ti}$	Cu	Ag-Cu eutectic	316L	Cu-rich

3.2. Microstructures of the Braze Joints

Phase identification using the EDS chemical analysis results was assisted by related phase diagrams and citing references. From Figure 3, Figure 5, Figure 6 and Tables 2–4, a continuous layer of the $(\text{Cu}_x\text{Ni}_{1-x})_2\text{Ti}$ intermetallic, as labelled by B, is formed at the interface between $\text{Ti}_{50}\text{Ni}_{50}$ substrate and Cusil-ABA filler. Based on Ti-Cu-Ni ternary phase diagram isothermally sectioned at

870 °C, the stoichiometric composition of this intermetallic layer is near the TiCuNi compound [19]. It is a nonstoichiometric compound, and can be indicated by $(\text{Cu}_x\text{Ni}_{1-x})_2\text{Ti}$ with x ranging from 0.23 to 0.75 [19]. The EDS chemical analyses of layer B indicated in Tables 2–4 are in accordance with Ti-Cu-Ni diagram [18].

From Figure 5b, there are two continuous layers observed at the interface between 316L SS and the braze. One is the Ti(Fe, Ni) intermetallic layer labelled by D, and the other is the (Fe, Cr)-rich layer indicated by E. Figure 7 illustrates the Fe-Ni-Ti phase diagram isothermally sectionalized at 900 °C [19,23]. The Ti₅₀Ni₅₀ substrate dissolved into the braze melt causes high Ni and Ti contents in it. The complete dissolution of 25 μm Cu barrier layer makes the Ti and Ni ingredients readily react with the 316L SS substrate in brazing, and yields a continuous reaction layer of Ti(Fe, Ni) intermetallic. According to Figure 7, the composition of layer D is regarded as the TiFe intermetallic compound alloyed with Ni. The layer E shown in Figure 5b, which is next to the 316L SS substrate, contains about 56% Fe, 22% Cr, 3% Ni, 9% Ag, and 10% Ti (in at %). The transport of Ti from the Ti₅₀Ni₅₀ substrate and Cusil-ABA melt now acts as an active brazing element to react with the surface of 316L SS substrate. Thereafter, Ti, Ag, and Ni atoms interact with 316L SS substrate to form a (Fe, Cr)-rich layer solid-solution alloyed with Ag, Ti, and Ni. In addition, some Ag atoms are not alloyed into (Fe, Cr)-rich phase, and form white Ag-rich precipitates in layer E (Figure 5b).

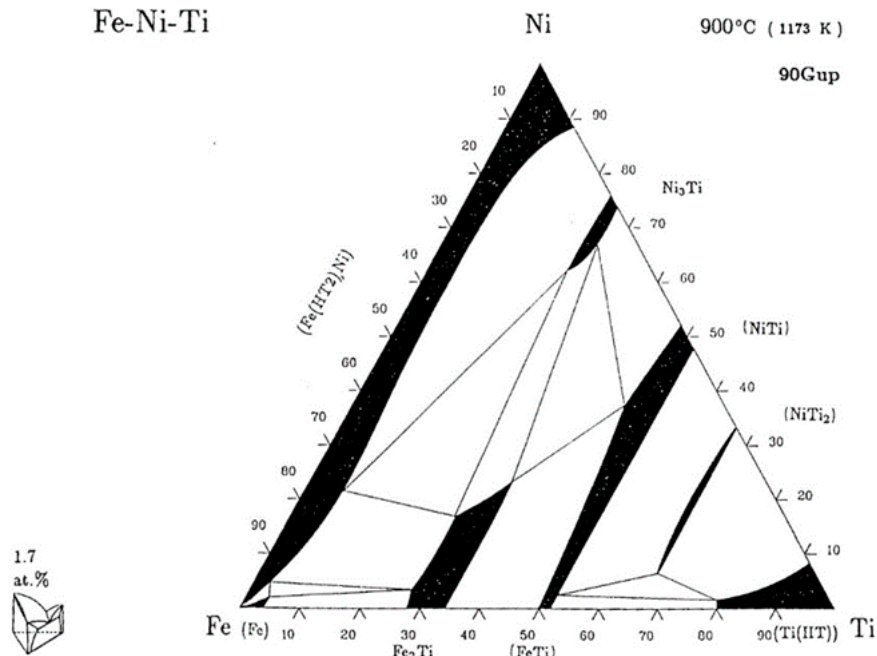


Figure 7. Isothermal section of Fe-Ni-Ti ternary phase diagram at 900 °C [19,23].

3.3. The Shear Strengths of Braze Joints

Table 5 indicates average shear strengths of the Ti₅₀Ni₅₀/Cusil-ABA/Cu foil/BAg-8/316L SS joints with different Cu barrier layers braze by infrared rays under different braze conditions. For comparison, the shear strengths of Ti₅₀Ni₅₀/Cusil-ABA or Ticusil/316L SS joint without the Cu barrier layer infrared braze at 870 °C for 300 s or at 950 °C for 60 s, respectively, are also tabulated [6]. From Table 5, average shear strengths of the specimens with 50 μm Cu foil can reach 354 MPa for braze at 820 °C for 300 s and 349 MPa for braze at 850 °C for 300 s. These values are significantly increased as compared with those without the Cu barrier layer, as indicated in Table 5.

Table 5. Average shear strengths of infrared brazed Ti₅₀Ni₅₀ SMA and 316L SS joints.

Filler Metal	Brazing Temperature	Brazing Time	Copper Foil Thickness	Average Shear Strength
Cusil-ABA/Cu foil/BAg-8	820 °C	300 s	25 µm	140 ± 3 MPa
			50 µm	354 ± 35 MPa
			70 µm	292 ± 37 MPa
	850 °C	300 s	25 µm	236 ± 38 MPa
			50 µm	349 ± 21 MPa
			70 µm	211 ± 39 MPa
Cusil-ABA *	870 °C	300 s	-	66 ± 15 MPa
Ticusil *	950 °C	60 s	-	237 ± 16 MPa

* From reference [6] in which the thickness of the filler metal is 50 µm.

All brazed joints failed along the interface between BAg-8 braze and 316L substrate. Figure 8a illustrates the cross-sectional results of SEM BEIs and the SEI fractograph of the fractured Ti₅₀Ni₅₀/Cusil-ABA/25 µm Cu foil/BAg-8/316L SS joined at 850 °C for 300 s. The brazed specimen failed along the interfacial reaction layer of Ti(Fe, Ni) (labelled by D in Figure 5b) next to the 316L SS substrate side. The SEM SEI fractograph shown in Figure 8a is features brittle fracture, and the EDS analysis result is consistent with that of layer D in Figure 5b. Figure 8b illustrates the cross-sectional results of SEM BEIs and the SEI fractograph of the fractured Ti₅₀Ni₅₀/Cusil-ABA/50 µm Cu foil/BAg-8/316L SS joined at 850 °C for 300 s. Different from Figure 8a, the fracture appearing in the brazed specimen is along the (Ag, Cu) eutectic (labelled by D in Figure 6b) near the 316L SS substrate side. The fracture of fine (Ag, Cu) eutectic, as shown in Figure 6b, results in many miniature dimples in Figure 8b. For the specimen with 70 µm Cu foil, the brazed joint is fractured along the (Ag, Cu) eutectic next to the 316L SS substrate side as shown in Figure 8c. A few solidification voids are observed from the fractured surface.

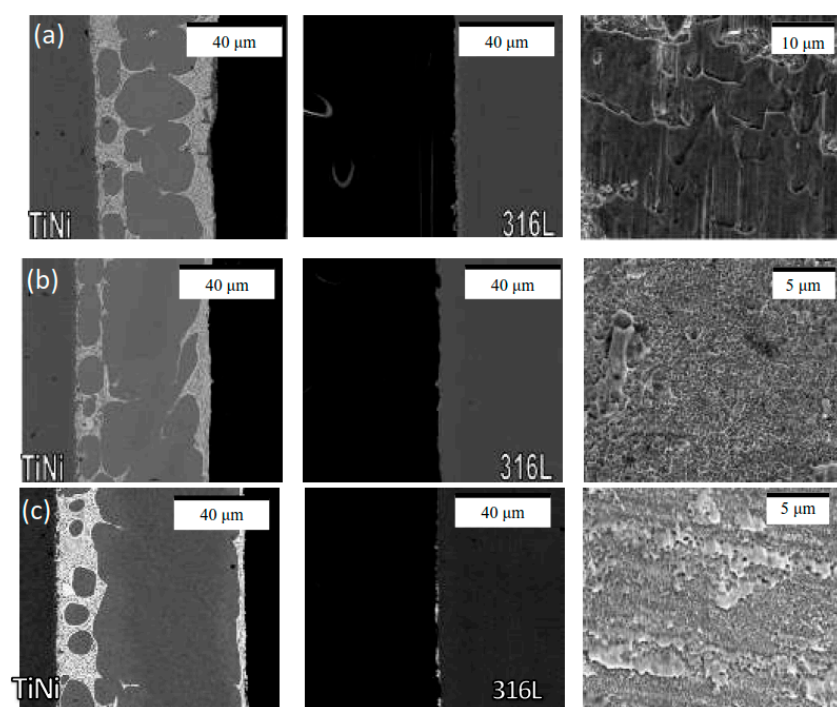


Figure 8. SEM BEI cross-sections and SEI fractographs of Ti₅₀Ni₅₀/Cusil-ABA/Cu foil/BAg-8/316L SS joint infrared brazed at 850 °C for 300 s after shear test with the Cu interlayer of (a) 25; (b) 50; and (c) 70 µm in thickness. (TiNi: Ti₅₀Ni₅₀ substrate, 316L: 316L SS substrate).

Shear strengths revealed in Table 5 indicate that the optimal thickness of the Cu barrier layer is 50 μm . The Cu barrier foil 25 μm in thickness is dissolved into the melt during brazing, and a continuous Ti(Fe, Ni) interfacial layer next to the 316L SS substrate side is formed which is the fracture location in shear test. In addition, the BAg-8 filler metal brazed at 820 $^{\circ}\text{C}$ is not high enough to sufficiently wet the 316L SS substrate. These reasons cause the brazed joint with 25 μm Cu foil to have a lower shear strength than that with 50 μm foil, especially the joint brazed at 820 $^{\circ}\text{C}$. Shear strength of the joint with 50 μm Cu foil demonstrates the highest joint strength due to the presence of very fine (Ag, Cu) eutectic and free of interfacial Ti(Fe, Ni) reaction layer. The shear strength of the joint with 70 μm Cu foil is lower than that of 50 μm one. The BAg-8 melt is easier to flow out of the joint during brazing than the Cusil-ABA one. The width of BAg-8 braze melt in 70 μm Cu foil is much less than that in 50 μm one, as compared between Figure 8b,c. Because solidification shrinkage voids are prone to be formed in the joint with the 70 μm Cu layer, the joint's shear strength is deteriorated. Shear test is the first stage in evaluating bonding strength of the brazed joint. Dynamic tests, such as fatigue testing, of such a brazed joint will be performed in the future in order to evaluate the effect of interfacial intermetallics on the reliability of the brazed joint.

4. Conclusions

Shear strength and microstructural evolution of Ti₅₀Ni₅₀ SMA/Cusil-ABA/Cu foil/BAg-8/316L SS joints brazed by infrared rays at 820 $^{\circ}\text{C}$ and 850 $^{\circ}\text{C}$ for 300 s with the Cu foil as the diffusion barrier have been investigated. The introduction of the Cu barrier layer shows great potential in joining Ti₅₀Ni₅₀ SMA and 316L SS for industrial application. Important conclusions are as follows:

1. The Cu foil serves as a barrier layer at thicknesses of 70 μm and 50 μm , and it successfully isolates the interfacial reaction between Ti and Fe at the 316L SS substrate side. In contrast, the Cu foil with 25 μm in thickness is completely dissolved into the braze melt during brazing and fails to be a barrier layer.
2. A layer of (Cu_xNi_{1-x})₂Ti intermetallic is formed at the Ti₅₀Ni₅₀ substrate side, and the Cu interlayer is dissolved into the Cusil-ABA melt to form a few proeutectic Cu particles for all specimens. For the 316L SS substrate side, no interfacial layer is observed and (Ag, Cu) eutectic dominates the brazed joint for 70 μm /50 μm Cu foil. However, an interfacial Ti(Fe, Ni) intermetallic layer and (Fe, Cr)-rich layer are formed in the brazed joint with the 25 μm Cu layer.
3. The joint with the 50 μm Cu barrier layer demonstrates the best average shear strengths of 354 MPa and 349 MPa for samples brazed at 820 $^{\circ}\text{C}$ and 850 $^{\circ}\text{C}$, respectively. All specimens are fractured along the interface between the BAg-8 braze and 316L SS side. Cracks are initiated/propagated in (Ag, Cu) eutectic for the 70 μm and 50 μm thickness Cu foils and at the interfacial Ti(Fe, Ni) reaction layer for the 25 μm foil. The formation of a brittle Ti(Fe, Ni) intermetallic layer deteriorates the bonding strength of the joint.

Acknowledgments: This research financial-supported from the Ministry of Science and Technology, Taiwan under grand number MOST 105-2221-E-002-044-MY2 was kindly acknowledged.

Author Contributions: Shyi-Kaan Wu and Ren-Kae Shiue designed and planned the experiment. Sheng-Hao Yang and Chun-Kai Liu made the test.

Conflicts of Interest: The authors announce no conflict of interest.

References

1. Funakubo, H. *Shape Memory Alloys*; Gordon & Breach Science: New York, NY, USA, 1987.
2. Otsuka, K.; Kakeshita, T. Science and technology of shape-memory alloys: New developments. *MRS Bull.* **2002**, *27*, 91–100. [[CrossRef](#)]
3. Braun, S.; Sandstrom, N.; Stemme, G.; Wijngaart, W. Wafer-scale manufacturing of bulk shape-memory-alloy microactuators based on adhesive bonding of titanium-nickel sheets to structured silicon wafers. *J. Microelectromech. Syst.* **2009**, *18*, 1309–1317. [[CrossRef](#)]

4. Tomozawa, M.; Kim, H.Y.; Miyazaki, S. Shape memory behavior and internal structure of Ti-Ni-Cu shape memory alloy thin films and their application for microactuators. *Acta Mater.* **2009**, *57*, 441–452.
5. Smith, W.F. *Structure and Properties of Engineering Alloys*; McGraw-Hill: New York, NY, USA, 1993; pp. 312–316.
6. Shiue, R.K.; Chen, C.P.; Wu, S.K. Infrared brazing $Ti_{50}Ni_{50}$ shape memory alloy and 316L stainless steel with two silver-based fillers. *Metall. Mater. Trans. A* **2015**, *46*, 2364–2371. [[CrossRef](#)]
7. Kumar, A.; Ganesh, P.; Kaul, R.; Sindal, B.K. New brazing recipe for ductile niobium-316L stainless steel joints. *Weld. J.* **2015**, *94*, 241–249.
8. Laik, A.; Shirzadi, A.A.; Sharma, G.; Tewari, R.; Jayakumar, T.; Dey, G.K. Microstructure and interfacial reactions during vacuum brazing of stainless steel to titanium using Ag-28 pct Cu alloy. *Metall. Mater. Trans. A* **2015**, *46*, 771–782.
9. Lee, M.K.; Park, J.J.; Lee, J.G.; Rhee, C.K. Phase-dependent corrosion of titanium-to-stainless steel joints brazed by Ag–Cu eutectic alloy filler and Ag interlayer. *J. Nucl. Mater.* **2013**, *439*, 168–173. [[CrossRef](#)]
10. Elrefaey, A.; Tillmann, W. Brazing of titanium to steel with different filler metals: Analysis and comparison. *J. Mater. Sci.* **2010**, *45*, 4332–4338. [[CrossRef](#)]
11. Lee, M.K.; Lee, J.G.; Lee, J.K.; Hong, S.M.; Lee, S.H.; Park, J.J.; Kim, J.W.; Rhee, C.K. Formation of interfacial brittle phases sigma phase and IMC in hybrid titanium-to-stainless steel joint. *Trans. Nonferrous Met. Soc. China* **2011**, *21*, 7–11. [[CrossRef](#)]
12. Liu, C.C.; Ou, C.L.; Shiue, R.K. The microstructural observation and wettability study of brazing Ti-6Al-4V and 304 stainless steel using three braze alloys. *J. Mater. Sci.* **2002**, *37*, 2225–2235. [[CrossRef](#)]
13. Morizono, Y.; Mizobata, A. Explosive coating of Ag-Cu filler alloy on metal substrates and its effect on subsequent brazing process. *ISIJ Int.* **2010**, *50*, 1200–1204. [[CrossRef](#)]
14. Lee, J.G.; Hong, S.J.; Lee, M.K.; Rhee, C.K. High strength bonding of titanium to stainless steel using an Ag interlayer. *J. Nucl. Mater.* **2009**, *395*, 145–149. [[CrossRef](#)]
15. Kamat, G.R. Solid-state diffusion welding of nickel to stainless steel. *Weld. J.* **1988**, *67*, 44–46.
16. He, P.; Zhang, J.H.; Zhou, R.L.; Li, X.Q. Diffusion bonding technology of a titanium alloy to a stainless steel web with a Ni interlayer. *Mater. Charact.* **1999**, *43*, 287–292. [[CrossRef](#)]
17. Shiue, R.K.; Wu, S.K.; Chan, C.H.; Huang, C.S. Infrared brazing Ti-6Al-4V and 17-4 PH stainless steel with a nickel barrier layer. *Metall. Mater. Trans. A* **2006**, *37*, 2207–2217. [[CrossRef](#)]
18. Massalski, T.B.; Okamoto, H.; Subramanian, P.R.; Kacprzak, L. Binary Alloy Phase Diagrams. In *ASM Metal Handbook*; ASM International: Geauga County, OH, USA, 1992; Volume 3, pp. 2–168.
19. Villars, P.; Prince, A.; Okamoto, H. *Handbook of Ternary Alloy Phase Diagrams*; ASM International: Geauga County, OH, USA, 1995.
20. Yang, S.H. *The Study of Infrared Brazing $Ti_{50}Ni_{50}$ SMA and 316L Stainless Steel/Inconel 600*; Department of Mechanical Engineering, National Taiwan University: Taipei, Taiwan, 2015; pp. 5–35.
21. Lee, S.J.; Wu, S.K.; Lin, R.Y. Infrared joining of TiAl intermetallics using Ti-15Cu-15Ni foil—Part I the microstructure morphologies of joint interfaces. *Acta Mater.* **1998**, *46*, 1283–1295. [[CrossRef](#)]
22. Shiue, R.K.; Chen, Y.H.; Wu, S.K. Infrared brazing $Ti_{50}Ni_{50}$ and invar using Ag-based filler foils. *Metall. Mater. Trans. A* **2013**, *44*, 4454–4460. [[CrossRef](#)]
23. Loo, F.; Vrolijk, J.; Bastin, G. Phase relations and diffusion paths in the Ti-Ni-Fe system at 900 °C. *J. Less-Common Met.* **1981**, *77*, 121–130.



© 2017 by the authors. Licensee MDPI, Basel, Switzerland. This article is an open access article distributed under the terms and conditions of the Creative Commons Attribution (CC BY) license (<http://creativecommons.org/licenses/by/4.0/>).